arXiv:cond-mat/0502411v1 [cond-mat.other] 17 Feb 2005

Probing Pair-Correlated Fermionic Atoms through Correlations in Atom Shot Noise

M. Greiner,* C. A. Regal, J. T. Stewart, and D. S. Jin†
JILA, National Institute of Standards and Technology and University of Colorado, and Department of Physics, University of Colorado, Boulder, CO 80309-0440
(Dated: February 2, 2008)

Pair-correlated fermionic atoms are created through dissociation of weakly bound molecules near a magnetic-field Feshbach resonance. We show that correlations between atoms in different spin states can be detected using the atom shot noise in absorption images. Furthermore, using time-of-flight imaging we have observed atom pair correlations in momentum space.

A variety of fascinating quantum systems have been realized with ultracold atoms over the past decade. A unique feature of these systems is that the quantum state is very accessible. Density distributions and matter waves can be directly probed in time-of-flight (TOF) expansion with absorption imaging [1]. This method has, for example, allowed observation of Bose-Einstein condensates (BEC), matter-wave interference patterns, and quantized vortices in the macroscopic matter wave. However, experiments are now beginning to access a further class of quantum systems that involve quantum entanglement and correlations. Examples include the Mott insulator state for atoms in an optical lattice [2, 3], proposed quantum Hall-like states for rapidly rotating condensates [4], and condensates of generalized Cooper pairs [5, 6, 7].

Altman *et al.* [8] recently pointed out that atom cloud absorption images can hold information beyond the first-order correlation provided by the density distribution. They proposed that density-density correlations can be directly measured by carefully analyzing the atom shot noise present in TOF absorption images of the atom gas. This analysis can reveal key properties of strongly correlated states of atoms such as fermionic superfluids or exotic states in optical lattices. The method of detecting two-particle correlations is reminiscent of the measurement of temporal current noise in mesoscopic conductors [9] and closely related to the detection of entangled photon pairs in quantum optics [10], which is fundamental to experiments studying nonclassical states of light.

Here we report on the creation and detection of local and nonlocal pairs of fermionic ^{40}K atoms. The pair-correlated atoms are created by dissociating weakly bound diatomic molecules near a Feshbach resonance and detected through the measurement of atom shot noise correlations in TOF absorption images. This novel detection method provides a new tool for probing highly correlated quantum states in atomic gases. In addition, pair-correlated atoms, such as demonstrated here, have uses in quantum information, precision measurements [11], and fundamental tests of quantum mechanics [12].

Measuring atom-atom correlations via the method proposed by Altman *et al.* [8] requires that atom shot noise dominates over other noise sources in absorption imaging. Atom shot noise arises because of the quantized nature of the atoms and causes a granularity in the observed density distribution (Fig. 1). In absorption imaging, the atoms scatter light out of a resonant laser beam, and the resulting shadow is imaged on a charge-coupled-device (CCD) camera [1]. The optical density is determined using $OD(\boldsymbol{r}) = \log(I_{\rm ref}(\boldsymbol{r})/I(\boldsymbol{r}))$, where $I(\boldsymbol{r})$ is the spatial intensity of the shadow image and $I_{\rm ref}(\boldsymbol{r})$ is a reference image taken with no atoms. The atom column density is given by $n(\boldsymbol{r}) = OD(\boldsymbol{r})/\sigma$, where $\sigma = 3\lambda^2/(2\pi)$ is the absorption cross section and λ is the wavelength of the imaging light. There can be three types of noise in these shadow images: atom shot noise, photon shot noise, and technical noise. Having a large photon number per pixel, N_p, in the absorption imaging beam keeps the technical noise of the CCD camera (dark current and readout noise) significantly smaller than the photon shot noise, $\delta N_p = \sqrt{N_p}$. Further, if each atom scatters a large number of photons, then the atom shot noise, $\delta N_a = \sqrt{N_a}$, will dominate over the photon shot noise [18].

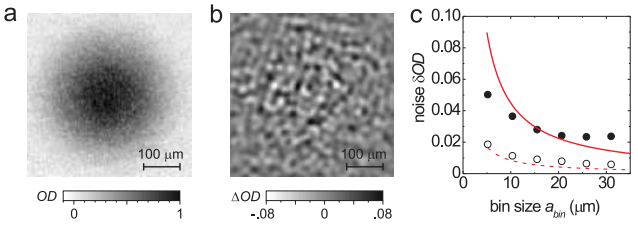

FIG. 1: Atom shot noise in a time-of-flight (TOF) absorption image. (a) One spin state of a weakly interacting, two-component, degenerate Fermi gas with 2.3×10^5 atoms per spin state is imaged after 19.2 ms of expansion. (b) The noise on the absorption image was extracted using a filter with an effective bin size of 15.5 microns. (c) The noise at the cloud center (•) is dominated by atom shot noise, while the noise at the edge of the image (○) shows the photon shot noise. The noise in OD decreases when averaged over a larger bin size. The predicted dependence for atom and photon shot noise is shown by the solid and dashed lines, respectively.

We image the atoms in the extremal $|f = 9/2, m_f = -9/2\rangle$ state using a cycling transition. With a laser intensity of 12% of the saturation intensity I_{sat}, the atoms each scatter, on average, 65 photons during our 40-μs

pulse. We use a back-illuminated CCD camera with a quantum efficiency of $QE = 80\%$. Additional losses on the imaging path give an overall quantum efficiency of about 70%. Figure 1(a) shows a raw absorption image of an atom cloud.

To extract the noise signal from the absorption image, $OD(\boldsymbol{r})$, we subtract an azimuthal average $\langle OD(r)\rangle$ from each pixel to get a raw noise image $\Delta OD(\boldsymbol{r}) = OD(\boldsymbol{r}) - \langle OD(r)\rangle$. In looking for atom shot noise, the size of the image pixels plays an important role. The atom number on a pixel or bin with area a_{bin}^2 is given by $N_a = \langle OD(r)\rangle\, a_{bin}^2/\sigma$. For Poissonian atom shot noise the magnitude of the fractional noise on a bin given by $\delta OD_{\rm atom}/OD = \sqrt{N_a}/N_a$ increases for smaller bins. However, if the bins are too small, the measured noise will be reduced by the fact that the absorption signal due to a single atom will be spread out over a finite area. In our experiment causes of this blurring include the imaging resolution ($\approx 5\,\mu$m), the random walk motion of the atoms because of photon scattering ($1\,\mu$m$-2\,\mu$m), and the falling motion of the cloud during the imaging pulse (up to $7.5\,\mu$m). To study the role of pixel size we can effectively vary the size of a bin for a given image by averaging over multiple camera pixels. We do this smoothly by applying a spatial low-pass filter with a variable cutoff spatial frequency $f_{\rm lp}$. In addition, we apply a high pass filter at a cutoff spatial frequency $f_{\rm hp} = f_{\rm lp}/4$ to eliminate technical noise that occurs at low spatial frequencies. For our filter (see [19]), a numerical simulation yields an effective bin size of $a_{bin} = 1.25/f_{\rm lp}$.

Figure 1(b) shows a processed noise image, and Fig. 1(c) demonstrates that atom shot noise can be the dominant noise source. For medium bin sizes, the measured noise at the cloud center ($OD{\approx}1$) is close to the expected atom shot noise. For small bin sizes, the noise is lower than expected. We attribute this to the blurring described above. For very large bin sizes, technical noise becomes more important, and the measured noise exceeds the expected atom shot noise. The measured background noise outside the atom cloud is only slightly larger than the expected photon shot noise, which is given by $\delta OD_{\rm photon} = \sqrt{1+e^{OD}}/\sqrt{N_p}$, where N_p is the photon number per effective bin.

The experiments probing pair-correlated atoms are initiated by trapping and cooling a dilute gas of fermionic ^{40}K atoms to ultralow temperatures [13, 14]. We initially prepare a nearly equal, incoherent mixture of atoms in the $|f, m_f\rangle = |9/2, -9/2\rangle$ and $|9/2, -7/2\rangle$ spin states, where f is the total spin and m_f the magnetic sublevel. The atoms, and the molecules we create from these atoms, are confined in a cigar-shaped far off-resonant optical dipole trap with radial trapping frequencies on the order of 300 Hz and an axial frequency of $\nu_z \approx \nu_r/70$.

Weakly bound molecules are created by tuning the interaction between atoms in the two spin states with a 7.8 ± 0.6 G [15] wide s-wave magnetic-field Feshbach resonance at 202.10 ± 0.07 G [5]. Slowly sweeping the magnetic field across the Feshbach resonance results in a pairwise conversion of $85 \pm 5\%$ of the atoms into molecules [16]. For adiabatic B-field ramps and our lowest temperatures, we get a Bose-Einstein condensate of molecules with typically 15% condensate fraction [5]. Pair-correlated atoms are then produced by dissociating the molecules with one of two techniques discussed below. The resulting atoms form an entangled singlet pair, with one atom in each of the two initial spin states. This entanglement follows from required exchange symmetry of the fermionic atoms and the s-wave nature of the interaction.

In a first experiment, we look for spatial atom-atom correlations by probing the gas immediately after the dissociation of weakly bound diatomic molecules. Here we ballistically expand a cloud of about 3×10^5 molecules for 19.2 ms. Then, we quickly dissociate the molecules into two atoms in the $m_f = -7/2$ and $m_f = -9/2$ states by increasing the magnetic field across the Feshbach resonance. Immediately after the dissociation, we image both spin states separately as described below. If the atoms do not move significantly relative to each other [20], the atom shot noise for the $m_f = -7/2$ and $m_f = -9/2$ images should be nearly identical.

To probe the singlet state, we need to independently measure atoms in two spin states quasi-instantaneously. This is done with a sequence of two pictures taken within $340\,\mu$s using a kinetics mode of the CCD camera. In the first absorption image only atoms in the $m_f = -9/2$ state are addressed. Because of a large Zeeman shift, absorption by atoms in other spin states is negligible. In the second picture, we selectively probe atoms in the $m_f = -7/2$ or $m_f = -5/2$ state by first flipping their spins to the extremal $m_f = -9/2$ state with one or two radio-frequency (rf) π-pulses, respectively, and then imaging in the $m_f = -9/2$ state. The Rabi rates for these rf transitions are, on average, $\Omega = 2\pi \times 30$ kHz.

Figure 2 shows that we can clearly observe the atom-atom correlations using the noise. We consider the correlation function $\mathcal{G}_{\alpha\beta}(\boldsymbol{r}, \boldsymbol{r'}) = \Delta N_\alpha(\boldsymbol{r})\Delta N_\beta(\boldsymbol{r'})$, where α and β denote the imaged spin states and $\Delta N_\alpha(\boldsymbol{r}) = \Delta OD_\alpha(\boldsymbol{r}) a_{bin}^2/\sigma$ is the fluctuation of atom number per bin, for atoms in spin state α. We calculate the correlation between atoms in the spin states α and β as a function of an angle representing a relative rotation about the cloud center. Specifically, we write the position in polar coordinates as $\boldsymbol{r} = (r, \phi)$ and $\boldsymbol{r'} = (r', \phi + \Delta\phi)$, centered on the cloud, and calculate the normalized correlation profile as

$$\tilde{\mathcal{G}}_{\alpha\beta}(\Delta\phi) = \left\langle \frac{\langle\, \Delta N_\alpha(r,\phi)\ \Delta N_\beta(r, \phi+\Delta\phi)\,\rangle_\phi}{\sqrt{\overline{N}_\alpha(r)\overline{N}_\beta(r)}} \right\rangle_r . \quad (1)$$

Here, $\overline{N}_\alpha(r)$ is the azimuthally averaged number of atoms in spin-state α per effective bin, and the correlations are

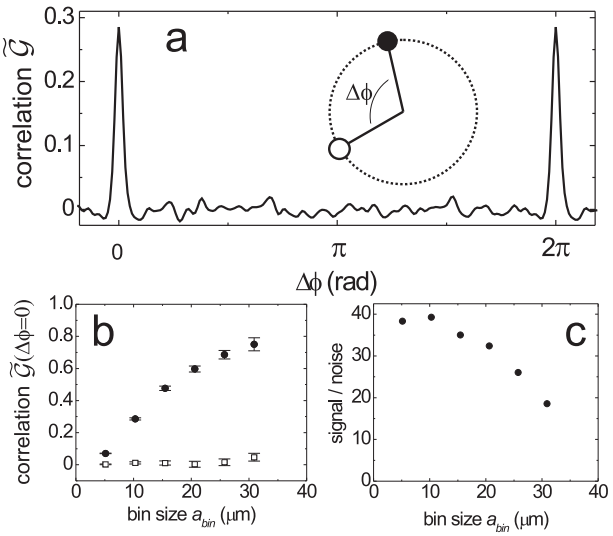

FIG. 2: Pair-correlated atoms. We plot the measured noise correlation as a function of a relative angle of rotation between absorption images of atoms in the two spin states (inset), averaged over 11 images. The effective bin size is 10.3 μm. Spatial pair correlations $\tilde{\mathcal{G}}_{\alpha\beta}(0)$ can clearly be seen when molecules are dissociated after expansion and then the atoms are immediately imaged [(a) and • in (b)]. The correlation signal disappears when the molecules are dissociated during an early stage of expansion [∘ in (b)]. By changing the low-pass filter to correspond to larger effective bin sizes, we measure a correlation signal as large as 75% (b). However, the signal-to-noise ratio in detecting the correlation is maximized for a lower effective bin size (c).

averaged over the angle ϕ, normalized, and then radially averaged. $\tilde{\mathcal{G}}_{\alpha\beta}(0)$ is the correlation between spin states α and β on identical points in space, and $\tilde{\mathcal{G}}_{\alpha\beta}(\pi)$ for diametrically opposite points. For perfect correlations $\Delta N_\alpha(r,\phi) = \Delta N_\beta(r,\phi+\Delta\phi)$ and Poissonian atom shot noise $\delta N_\alpha = \sqrt{\overline{N}_\alpha}$, the correlation function $\tilde{\mathcal{G}}_{\alpha\beta}(\Delta\phi)$ is unity.

If the molecules are dissociated immediately before imaging, we find a clear positive correlation signal for $\Delta\phi = 0$ [Fig. 2(a)]. In looking at the dependence of the correlation peak on the effective bin size in Figs. 2(b) and 2(c), we find that a small bin size is optimal for detecting the presence of correlations, while a larger bin size is necessary to accurately measure the amount of correlation. We find the largest correlation signal of 0.75 for our largest bin sizes [21], which is close to an expected signal of 0.85 for our $85 \pm 5\%$ molecule conversion efficiency. The lower signal for smaller bins indicates that the correlations are spread out over a finite area in the images. One cause of this could be the relative motion of atoms in the time between dissociation and imaging of the second spin state. Indeed, we find no correlations if we dissociate the atoms immediately after the start of TOF expansion [Fig. 2(b)]. On the other hand, the signal-to-noise ratio for detecting the presence of the pair correlations, defined as the ratio of $\tilde{\mathcal{G}}_{\alpha\beta}(0)$ to the standard deviation of $\tilde{\mathcal{G}}_{\alpha\beta}(\Delta\phi \neq 0)$, is maximized for a significantly smaller effective bin size. This is because smaller bins have larger fractional atom number noise and one has more pixel pairs over which to average the correlation signal. The width of the correlation peaks is limited by the effective bin size and the blurring of the correlations.

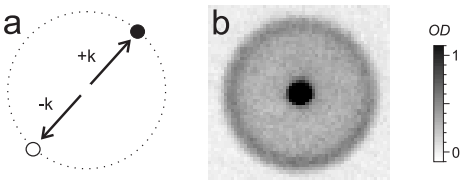

FIG. 3: (a) Atoms with equal but opposite momentum are found on opposite sides of the atom cloud in TOF expansion. (b) This atom absorption image was taken after rf photodissociation of weakly bound molecules using an rf detuning of $\Delta\nu_{rf} = 1.3$ MHz. The pair-correlated atoms comprise an expanding spherical shell, containing approximately 1.3×10^5 atoms per spin state, which appears as a ring in the 2D absorption image.

In a second experiment, we are able to detect nonlocal pair correlations between atoms that have equal but opposite momentum and are therefore found at diametrically opposite points of the atom cloud in TOF expansion [Fig. 3(a)]. These pair correlations are created by dissociation of molecules in the optical trap and expansion of the atom gas before imaging. A significant further experimental challenge arises from the fact that any center-of-mass motion of the pairs rapidly degrades the correlation signal due to blurring. We use several strategies to minimize this effect. First, we start with an ultracold molecule sample. Second, although we start with molecules in the strongly interacting regime at $B = 202.07$ G, we rapidly change the B-field to 198 G (within 50 μs) before dissociation to avoid strong interaction effects during the expansion. Third, we dissociate the molecules to non-zero relative momentum states using rf photodissociation [17].

Detuning the rf with respect to the atomic transition by $\Delta\nu_{rf} + E_{binding}$ results in free atoms (now in the $m_f = -9/2$ and $m_f = -5/2$ spin-states) that fly apart in opposite directions with a relative momentum of $p = \sqrt{m\,h\,\Delta\nu_{rf}}$. By increasing the rf detuning, we can give the atoms a relative momentum that is much larger then their center-of-mass momentum [Fig. 3(b)]. In the TOF images, we expect $\tilde{\mathcal{G}}_{(-5/2,-9/2)}(\Delta\phi)$ to show positive correlation at $\Delta\phi = \pi$.

Figure 4(b) shows example absorption images used to find nonlocal correlations in the experiment. Here the

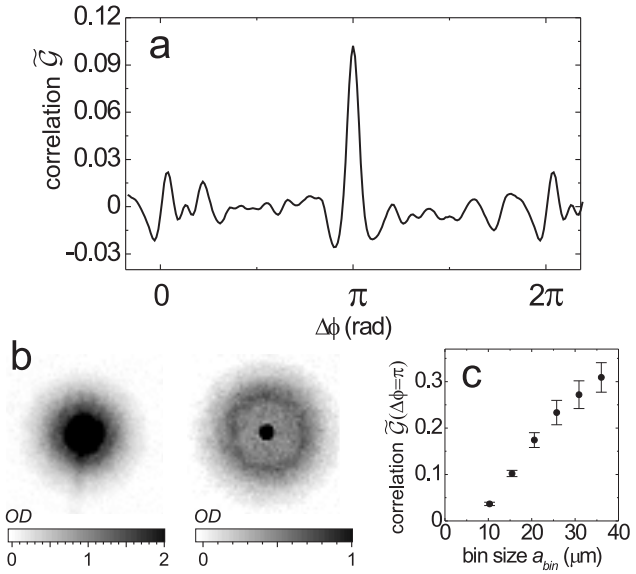

FIG. 4: Atom pair correlations in momentum space. (a) The averaged correlation signal for 102 image pairs shows a peak for atoms with equal but opposite momentum. The effective bin size is 15.5 μm. (b) TOF absorption images of atoms in the two spin-states, taken after 1.4 ms and 1.7 ms. (c) For large effective bins, we observe a correlation signal as high as 30%. The signal-to-noise ratio is on the order of 10.

molecules are dissociated using a 330-μs rf pulse with an average rf detuning of $\Delta\nu_{rf} = 1.1$ MHz beyond the dissociation threshold. In order to spread the dissociation shell over more camera pixels, we sweep the rf over 600 kHz. The absorption images are then taken after only 1.4 ms and 1.7 ms of expansion. Before calculating the correlation signal, we radially scale the second image to account for the additional expansion time. Figure 4(a) shows a correlation signal $\tilde{\mathcal{G}}_{(-5/2,-9/2)}(\Delta\phi)$ averaged for 102 images [22]. The clear peak at $\Delta\phi = \pi$ corresponds to nonlocal correlations in position, which are a result of correlations in momentum space. We find that including a BEC in our ultracold molecular sample does not significantly increase the correlation strength.

With a similar method [8], it seems feasible to directly probe generalized Cooper pairs in the BCS-BEC crossover region [5, 6, 7]. These pairs would be detected as momentum correlations in the same way as presented here. For this measurement, it will be important to maximize the ratio between the relative and the center-of-mass momentum of the dissociated pairs and minimize the collision rate during the initial stage of TOF expansion. In the experiments we have done thus far we find that the magnitude of the correlation signal critically depends on these two parameters.

In conclusion, we have demonstrated that analysis of the noise in absorption imaging can be used to directly probe atom-atom correlations in a quantum gas. Here we have been able to detect both local and nonlocal atom pair correlations created by the dissociation of weakly bound singlet molecules. The new method presented here will allow probing of interesting many-body states such as Cooper pairs in an atomic Fermi gas as well as antiferromagnetic phases and spin waves in optical lattices [8].

We would like to thank Ehud Altman for fruitful discussions and Jason Smith for experimental assistance. This work was supported by NSF and NASA. C. A. R. acknowledges support from the Hertz Foundation.

* Email: markus.greiner@colorado.edu; URL:http://jilawww.colorado.edu/~jin/
† Quantum Physics Division, National Institute of Standards and Technology.

[1] M. H. Anderson *et al.*, Science **269**, 198 (1995).
[2] D. Jaksch *et al.*, Phys. Rev. Lett. **82**, 1975 (1999).
[3] M. Greiner *et al.*, Nature **415**, 39 (2002).
[4] N. R. Cooper, N. K. Wilkin, and J. M. F. Gunn, Phys. Rev. Lett. **87**, 120405 (2001).
[5] C. A. Regal, M. Greiner, and D. S. Jin, Phys. Rev. Lett. **92**, 040403 (2004).
[6] M. W. Zwierlein *et al.*, Phys. Rev. Lett. **92**, 120403 (2004).
[7] C. Chin *et al.*, Science **305**, 1128 (2004).
[8] E. Altman, E. Demler, and M. D. Lukin, Phys. Rev. A **70**, 013603 (2004).
[9] Y. M. Blanter and M. Buttiker, Phys. Rep. **336**, 1 (2000).
[10] See, e.g. M. O. Scully and M. S. Zubairy, *Quantum Optics* (Cambridge University Press, Cambridge, 1997).
[11] C. Orzel *et al.*, Science **291**, 2386 (2001).
[12] E. S. Fry, T. Walther, and S. Li, Phys. Rev. A **52**, 4381 (1995).
[13] C. A. Regal and D. S. Jin, Phys. Rev. Lett. **90**, 230404 (2003).
[14] B. DeMarco and D. S. Jin, Science **285**, 1703 (1999).
[15] C. A. Regal, C. Ticknor, J. L. Bohn, and D. S. Jin, Phys. Rev. Lett. **90**, 053201 (2003).
[16] E. Hodby *et al.*, cond-mat/0411487 .
[17] C. A. Regal, C. Ticknor, J. L. Bohn, and D. S. Jin, Nature **424**, 47 (2003).
[18] It is important to minimize technical noise from interference patterns in the imaging laser beam. Interference is canceled by normalization to a reference image with no atoms. To optimize the normalization, we use a relatively clean imaging beam, take the normalization image only 4 ms after the original image, and image with a cycling transition at an appropriate light level.
[19] After a 2D Fourier transform, a Butterworth Bandpass filter function $\left(1+(f/f_{\rm lp})^{2n}\right)^{-1} - \left(1+(f/f_{\rm hp})^{2n}\right)^{-1}$ is applied, where $n = 5$ is the filter order and f is the norm of the spatial frequency. Then the image is transformed back to real space, simultaneously increasing the image resolution by interpolation.
[20] The atoms move vertically because of gravity between

the two images. We separately determine the cloud center with a 2D surface fit in both pictures.
[21] The correlation signal has a relative systematic uncertainty of $\approx 25\,\%$ because of the uncertainty in measuring the absolute atom number.
[22] To further optimize the signal-to-noise ratio, we have subtracted off the technical correlations that are constant over all images. These are determined by first averaging the 102 images and then calculating the remaining correlation signal.